archives
of thermodynamics
Vol. **44**(2023), No. 4, 563–579
DOI: 10.24425/ather.2023.149735

The analysis of the stability of the Cauchy problem in the cylindrical double-layer area

MICHAŁ CIAŁKOWSKI[a]
MAGDA JOACHIMIAK[a*]
MAGDALENA MIERZWICZAK[b]
ANDRZEJ FRĄCKOWIAK[b]
ALEKSANDER OLEJNIK[c]
ADAM KOZAKIEWICZ[c]

[a] Poznan University of Technology, Institute of Thermal Engineering, Piotrowo 3a, 60-965, Poznań, Poland

[b] Poznan University of Technology, Institute of Applied Mechanics, Jana Pawła II 24, 60-965, Poznań, Poland

[c] Military University of Technology, Sylwestra Kaliskiego 2, 00-908 Warszawa, Poland

Abstract Ceramic protective coats, for instance, on turbine blades, create a double-layer area with various thermophysical properties and they require metal temperature control. In this paper, it is implemented by formulating a Cauchy problem for the equation of thermal conductivity in the metal cylindrical area with a ceramic layer. Due to the ill posed problem, a regularization method was applied consisting in the notation of thermal balance for the ceramic layer. A spectral radius for the equation matrix was taken as the stability measure of the Cauchy problem. Numerical calculations were performed for a varied thickness of the ceramic layer, with consideration of the non-linear thermophysical properties of steel and a ceramic layer (zirconium dioxide). A polynomial was determined which approximates temperature distribution in time for the protective layer. The stability of solutions was compared for undisturbed and disturbed temperature values, and thermophysical parameters with various ceramic layer thickness. The obtained calculation results confirmed the effectiveness of the proposed regularization method in obtaining stable solutions at random data disturbance.

*Corresponding Author. Email: magda.joachimiak@put.poznan.pl

Keywords: Cauchy problem; Quasiregularization method; Protective layer; Cylindrical double-layer area

Nomenclature

c	–	specific heat, J/kgK
div	–	divergence
g	–	metal layer thickness, m
q	–	heat flux, W/m^2
r	–	radius, m
T	–	temperature, °C
t	–	time, s
x	–	dimensionless coordinate

Greek symbols

Γ	–	boundary
δ_c	–	thickness of ceramic, m
$\tilde{\delta}$	–	relative error, %
λ	–	thermal conductivity, W/mK
λ_s	–	spectral radius of stability matrix
ρ	–	density, kg/m^3
Ω	–	area
∇	–	gradient

Subscripts

c	–	ceramic, the outer surface of the ceramic
in	–	inner surface of the metal
m	–	metal
out	–	outer surface of the metal
s	–	specific heat
stab	–	stability matrix

1 Introduction

The efficiency of the gas turbine circulation depends, inter alia, on the temperature and pressure of gas flowing out from the combustion chamber [1–5], and their values are limited by the thermal resistance of the washed surface [6]. In order to prevent the blade metal from exceeding a given temperature, cooling channels [7–9] are made in such a blade or a thin ceramic layer is applied on its surface, which is characteristic for high thermal resistance (low value of a thermal conductivity coefficient) [10–12]. Assuming the equality of temperature and heat flux at the metal-ceramic contact point, with an unknown temperature on the outer ceramic surface leads to the Cauchy problem [10–14]. The problem of inverse thermal conductivity for double-layer areas may also be applied in the analysis of the heat loads of boilers [15–17], heat exchanger pipes with sediment [18], small arms barrels [19] or orbiter skin [20].

Inverse problems are regarded as ill posed in Hadamard sense [21–26], and the solution may be highly sensitive to the input data errors [27–30]. This is particularly important if inverse calculations involve experimental data burdened with a random measurement error [31–35]. Even small data errors may lead to huge errors in solutions which makes inverse problems difficult to solve numerically. Nevertheless, the majority of the existing numerical methods may provide stable solutions for boundary-initial problems by use of regularization techniques [36–38]. Those most popular include: Tikhonov regularization method [39], singular value decomposition method [40], statistical Bayesian inference, gradient-based regularization algorithm, entropy maximum. The regularization methods may need an additional parameter for which the determination of a value poses an additional challenge. One of the optimal parameter selection criteria is a discrepancy principle, L-curve criterion or the generalized cross-validation (GCV) [41,42].

In this paper, as a regularization method which does not require introducing any additional parameters, a notation of energy balance is used for the ceramic layer covering a metal surface [10]. Whereas, the spectral radius of the equation matrix [43] was used for the stability analysis of the proposed calculation model. The first part of the paper includes the demonstration of the solution model for the Cauchy problem for thermal conductivity in the cylindrical double-layer area. The second part includes the presentation of the numerical calculation results, with particular attention given to solution stability with the various geometry parameters of the tested area.

2 Cauchy problem

The calculations were carried out for the double-layer cylindrical area which is presented in Fig. 1. Thermal conductivity takes place in the metal layer for radii $r \in \langle r_{\text{in}}, r_{\text{out}} \rangle$ and in the ceramic layer for radii $r \in \langle r_{\text{out}}, r_c \rangle$. The metal layer thickness is $g = r_{\text{out}} - r_{\text{in}}$ and the ceramic layer thickness is $\delta_c = r_c - r_{\text{out}}$. Thermal conductivity coefficient, density and specific heat for metal are defined as λ_m, ρ_m, c_m, respectively, and for the ceramic, these are λ_c, ρ_c, and c_c.

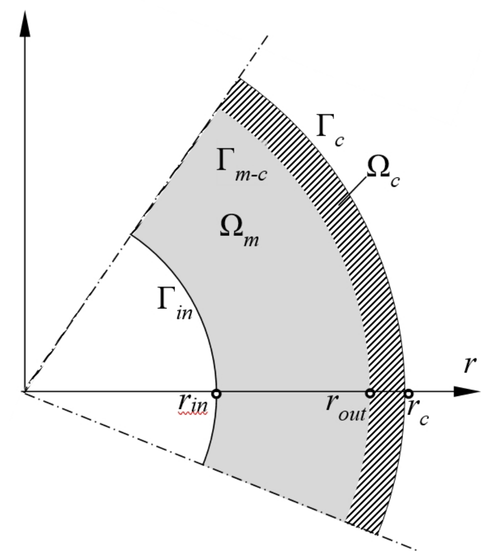

Figure 1: The calculation area consisting of the metal and ceramic layer.

The solution of the Cauchy problem considers an equation for thermal conductivity in the metal layer

$$\rho_m c_m \frac{\partial T_m}{\partial t} = \operatorname{div}\left(\lambda_m \nabla T_m\right), \quad r \in \langle r_{\text{in}}, r_{\text{out}} \rangle, \quad t > 0 \tag{1}$$

and in the ceramic layer

$$\rho_c c_c \frac{\partial T_c}{\partial t} = \operatorname{div}\left(\lambda_c \nabla T_c\right), \quad r \in \langle r_{\text{out}}, r_c \rangle, \quad t > 0. \tag{2}$$

The initial condition was assumed for $t = 0$ for the following the form:

$$T(r, 0) = f(r), \quad r \in \langle r_{\text{in}}, r_c \rangle. \tag{3}$$

On the metal inner surface Γ_{in} (for $r = r_{\text{in}}$) the boundary condition was accepted as

$$T(r_{\text{in}}, t) = T_0(t). \tag{4}$$

On the metal-ceramic contact point Γ_{m_c} (for $r = r_{\text{out}}$) the condition of the conformity of temperature and heat fluxes was accepted as

$$T_m(r_{\text{out}}, t) = T_c\left(r_{\text{out}}, t\right) = T_g(t), \tag{5}$$

$$\lambda_m \frac{\partial T_m\left(r_{\mathrm{out}}, t\right)}{\partial r} = \lambda_c \frac{\partial T_c\left(r_{\mathrm{out}}, t\right)}{\partial r}\,. \tag{6}$$

The solution of the thermal conductivity equation (2) for the ceramic area Ω_c with initial (3) and boundary (5) and (6) conditions is the Cauchy problem which is an ill posed problem [22]. The problem with the stability of the inverse problems solution necessitates the use of regularization [13, 38, 44, 45]. This paper does not include a classic regularization method [36, 37, 39, 40] but quasiregularization consisting in the consideration of the energy equation in the ceramic area Ω_c. The energy balance equation in the ceramic area Ω_c was obtained by integrating Eq. (2):

$$\begin{aligned}\int\limits_{r_{\mathrm{out}}}^{r_c} \rho_c(T) c_c(T) \frac{\partial T}{\partial t}\, dr &= \lambda_c \left[T(r,t)\right] \left.\frac{\partial T(r,t)}{\partial r}\right|_{r=r_c} - \lambda_c \left[T(r,t)\right] \left.\frac{\partial T(r,t)}{\partial r}\right|_{r=r_{\mathrm{out}}} \\ &= q_c(t) - q_{\mathrm{out}}(t) = \delta q. \end{aligned} \tag{7}$$

The heat conduction equations for metal (1) and ceramics (2) differ in the values of the thermophysical coefficients (λ, ρ, c). In the following analysis, the subscripts denoting metal (m) and ceramics (c) are omitted. Thus, we consider an equation of the form

$$\rho(T) c(T) \frac{\partial T}{\partial t} = \operatorname{div}\left[\lambda(T) \nabla T\right]. \tag{8}$$

By solving the non-linear Eq. (8) for a given unit of time, iterative calculations were performed to determine the correlated temperature and thermophysical coefficients more accurately, according to the following scheme:

$$\rho\left(T^m\right) c\left(T^m\right) \frac{\partial T^{m+1}}{\partial t} = \operatorname{div}\left[\lambda\left(T^m\right) \nabla T^{m+1}\right], \quad m = 1, 2, \ldots \tag{9}$$

The iterative process was terminated when the inequality was satisfied

$$\left\| T^{m+1} - T^m \right\| < \varepsilon \tag{10}$$

for a given value of $\varepsilon > 0$. The derivative after time $\frac{\partial T}{\partial t}$ was approximated by the backward differential quotient for consecutive moments of time t_{n+1} and t_n. The differential operation on the right-hand side of Eq. (9) was performed. Thus, the following was obtained:

$$\begin{aligned}\rho\left(T^n\right) c\left(T^n\right) \frac{T^{n+1} - T^n}{\Delta t} &= \lambda\left(T^n\right) \left(\frac{d^2 T^{n+1}}{dr^2} + \frac{1}{r} \frac{dT^{n+1}}{dr} \right) \\ &\quad + \lambda'\left(T^n\right) \frac{dT^n}{dr} \frac{dT^{n+1}}{dr} \end{aligned} \tag{11}$$

for $r \in \Omega_m$ or $r \in \Omega_c$. Using the central differential quotients at point r_i for the right-hand side of Eq. (11) for time t_{n+1} we obtain the differential form of Eq. (9):

$$\begin{aligned} &\rho\left(T_i^n\right) c\left(T_i^n\right) \frac{T_i^{n+1}-T_i^n}{\Delta t} \\ &\qquad = \frac{\lambda\left(\frac{T_{i+1}^n+T_i^n}{2}\right) \frac{T_{i+1}^{n+1}-T_i^{n+1}}{r_{i+1}-r_i} - \lambda\left(\frac{T_i^n+T_{i-1}^n}{2}\right) \frac{T_i^{n+1}-T_{i-1}^{n+1}}{r_i-r_{i-1}}}{\frac{r_{i+1}+r_i}{2}-\frac{r_i+r_{i-1}}{2}} \\ &\qquad\quad + \frac{\lambda\left(T_i^n\right)}{r_i} \cdot \frac{T_{i+1}^{n+1}-T_{i-1}^{n+1}}{r_{i+1}-r_{i-1}} + \lambda'\left(T_i^n\right) \frac{T_{i+1}^n-T_{i-1}^n}{r_{i+1}-r_{i-1}} \cdot \frac{T_{i+1}^{n+1}-T_{i-1}^{n+1}}{r_{i+1}-r_{i-1}}, \\ &\qquad\quad i=1,2,\ldots \end{aligned} \tag{12}$$

Finally, an equation was obtained as follows for each internal point of the area of metal Ω_m and ceramic Ω_c we have

$$a_{i,i-1} T_{i-1}^{n+1} + a_{i,i} T_i^{n+1} + a_{i,i+1} T_{i+1}^{n+1} = b_i T_i^n . \tag{13}$$

The coefficients $a_{i,i-1}$, $a_{i,i}$, $a_{i,i+1}$, and b_i contain the values of the thermo-physical coefficients and temperature at time t_n. The nodes adopted in the calculations for the metal and ceramic layers are shown in Fig. 2.

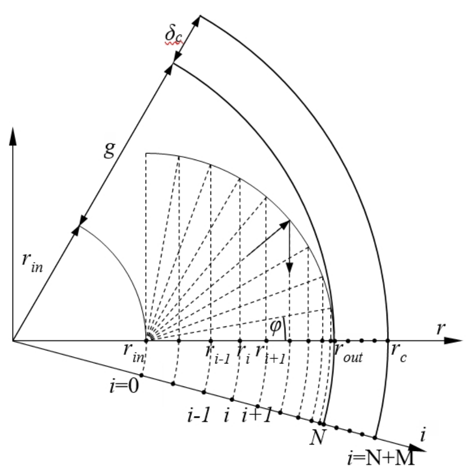

Figure 2: Nodes of a two-layer area.

After using discretization for Eqs. (1) and (2) of the conditions (3)–(6) and the trapezoidal integration of Eq. (7) the problem is reduced to the matrix equation of the form for time t_{n+1}:

$$[\alpha^n] \left\{T^{n+1}\right\} = [\beta^n] \{T^n\}. \tag{14}$$

The temperature at consecutive nodes $i = 0, 1, 2, \ldots, N+M$ (as shown in Fig. 2) for time t_n and t_{n+1} was described by vectors of the form

$$\{T^n\} = \left\{T_0^n, T_1^n, \ldots, T_{N+M}^n\right\}^T, \tag{15}$$

$$\left\{T^{n+1}\right\} = \left\{T_0^{n+1}, T_1^{n+1}, \ldots, T_{N+M}^{n+1}\right\}^T. \tag{16}$$

The matrices $[\alpha^n]$ and $[\beta^n]$ written for the metal and ceramic areas supplemented by the initial condition (3), the temperature (5) and heat flux compatibility conditions (6) and the energy balance equation (7) in the ceramic layer at time t_{n+1} after performing the differentiation operation of the non-linear equation according to Eqs. (11)–(12). Hence

$$[\alpha^n] = \begin{bmatrix} A_m^n \\ A_c^n \\ \text{equality of temperature, Eq. (5)} \\ \text{equality of heat flux, Eq. (6)} \\ \text{energy balance, Eq. (7)} \end{bmatrix}. \tag{17}$$

The computational model, together with Eq. (14), is described in detail in [46]. A novelty in the present work is the analysis of the stability of the computational method using the spectral radius, as described later in the paper. Equation (14) can be translated into the form

$$\begin{aligned}[A^n] \left\{T^{n+1}\right\} = [\beta^n] \{T^n\} &- \left\{\alpha_{00}^n, \alpha_{10}^n, \ldots, \alpha_{N+M,0}^n\right\}^T T_0^{n+1} \\ &- \left\{\alpha_{0N}^n, \alpha_{1N}^n, \ldots, \alpha_{N+M,N}^n\right\}^T T_g^{n+1}.\end{aligned} \tag{18}$$

The matrix $[A^n]$ is formed from the matrix $[\alpha^n]$ by transferring the values obtained from the known temperature T_0^{n+1} and T_g^{n+1} to the right-hand side of the equation. In Eq. (18) T_0^{n+1} is the temperature for radius $r = r_{\text{in}}$, while T_g^{n+1} is the temperature at the metal-ceramic interface for radius $r = r_{\text{out}}$ (according to Eq. (5)) for time t_{n+1}. Multiplying Eq. (18) by the matrix $[A^n]^{-1}$ on both sides, the following was obtained:

$$\begin{aligned}\left\{T^{n+1}\right\} &= [A^n]^{-1}[\beta^n]\{T^n\} - [A^n]^{-1}\left\{\alpha^n_{00}, \alpha^n_{10}, \ldots, \alpha^n_{N+M,0}\right\}^T T_0^{n+1} \\ &\quad - [A^n]^{-1}\left\{\alpha^n_{0N}, \alpha^n_{1N}, \ldots, \alpha^n_{N+M,N}\right\}^T T_g^{n+1} \\ &= [A^n_{\text{stab}}]\{T^n\} + \{c^n\} T_0^{n+1} + \{d^n\} T_g^{n+1} \\ &= [A^n_{\text{stab}}]\{T^n\} + \{e^n\}. \end{aligned} \tag{19}$$

where the matrix $[A^n_{\text{stab}}] = [A^n]^{-1}[\beta^n]$. The subscript "stab" is used to denote the matrix, the spectral radius of which is the measure of the stability of the solution of the inverse problem under consideration.

Thus, for successive moments of time, we have:

$$n = 0: \quad \left\{T^1\right\} = \left[A^0_{\text{stab}}\right]\left\{T^0\right\} + \left\{e^0\right\}, \tag{20}$$

$$\begin{aligned} n = 1: \quad \left\{T^2\right\} &= \left[A^1_{\text{stab}}\right]\left\{T^1\right\} + \left\{e^1\right\} \\ &= \left[A^1_{\text{stab}}\right]\left[A^0_{\text{stab}}\right]\left\{T^0\right\} + \left[A^1_{\text{stab}}\right]\left\{e^0\right\} + \left\{e^1\right\}, \end{aligned} \tag{21}$$

$$\begin{aligned} n = 2: \quad \left\{T^3\right\} &= \left[A^2_{\text{stab}}\right]\left\{T^2\right\} + \left\{e^2\right\} \\ &= \left[A^2_{\text{stab}}\right]\left[A^1_{\text{stab}}\right]\left[A^0_{\text{stab}}\right]\left\{T^0\right\} + \left[A^2_{\text{stab}}\right]\left[A^1_{\text{stab}}\right]\left\{e^0\right\} \\ &\quad + \left[A^2_{\text{stab}}\right]\left\{e^1\right\} + \left\{e^2\right\}, \end{aligned} \tag{22}$$

$$\begin{aligned} n = 3: \quad \left\{T^4\right\} &= \left[A^3_{\text{stab}}\right]\left\{T^3\right\} + \left\{e^3\right\} \\ &= \left[A^3_{\text{stab}}\right]\left[A^2_{\text{stab}}\right]\left[A^1_{\text{stab}}\right]\left[A^0_{\text{stab}}\right]\left\{T^0\right\} \\ &\quad + \left[A^3_{\text{stab}}\right]\left[A^2_{\text{stab}}\right]\left[A^1_{\text{stab}}\right]\left\{e^0\right\} + \left[A^3_{\text{stab}}\right]\left[A^2_{\text{stab}}\right]\left\{e^1\right\} \\ &\quad + \left[A^3_{\text{stab}}\right]\left\{e^2\right\} + \left\{e^3\right\} \end{aligned} \tag{23}$$

and, in general, for a linear issue, $\left[A^k_{\text{stab}}\right] = [B_{\text{stab}}] = \text{const}$. Then, for $n = k$ the equality occurs

$$\left\{T^{k+1}\right\} = [B_{\text{stab}}]^{k+1}\left\{T^0\right\} + \sum_{j=0}^{k}[B_{\text{stab}}]^{k-j}\left\{e^j\right\}. \tag{24}$$

For $k \to \infty$ if the spectral radius of the matrix $[B_{\text{stab}}]$, $\lambda_s([B_{\text{stab}}]) < 1$, then series (24) converges, while the first term tends towards zero (the initial condition at successive moments of time has less and less influence on the solution of the inverse problem). Therefore, for the convergence of the solution of a nonlinear problem at successive moments of time, the inequality must exist

$$\lambda_s\left(\left[A^k_{\text{stab}}\right]\right) < 1. \tag{25}$$

3 Numerical calculations

The essence of numerical calculations is demonstrating the impact of the ceramic coat thickness δ_c on the outer surface of the circular ring with the set geometry (inner radius $r_{\text{in}} = 50$ mm and outer radius $r_{\text{out}} = 100$ mm) on the value of the temperature on the ceramic surface. At the same time, it is assumed that temperature $T_{mc} = 686°$C on the metal-ceramic contact point will not be exceeded. When using the ceramic layer with the thickness of $\delta_c = 0.1$ mm the temperature on the outer ceramic surface was 918.6°C after the heating time of 100 s and not exceeding the assumed temperature T_{mc}. For the ceramic thickness $\delta_c = 0.2$ mm and $\delta_c = 0.3$ mm, the temperature on the outer ceramic surface was 1177.3°C and 1469.4°C, respectively (Fig. 3). These values indicate that surfaces of e.g. a gas turbine blade with a ceramic layer may operate in the conditions of significantly higher heat loads than without a protective coat.

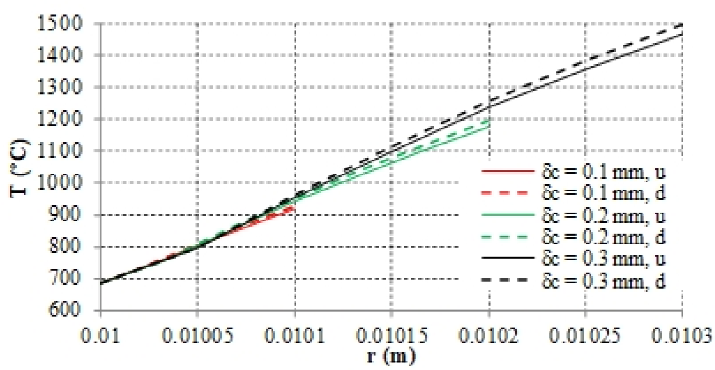

Figure 3: Temperature distribution in the ceramic layer after 100 s for the different thickness of the ceramic layer ($\delta_c = 0.1$ mm, $\delta_c = 0.2$ mm, and $\delta_c = 0.3$ mm) with disturbed (d) and undisturbed (u) input data.

In the subsequent numerical test, the temperature on the metal-ceramic contact point was disturbed randomly to the value of $\tilde{\delta}_T = 0.5\%$. The calculations were conducted with consideration of the non-linear thermophysical properties of metal and ceramic (thermal conductivity coefficient (λ), density (ρ) and specific heat (s)). The calculations were performed for the random disturbances of thermophysical parameters with the value of $\tilde{\delta}_{\lambda m} = \tilde{\delta}_{\rho m} = \tilde{\delta}_{sm} = \tilde{\delta}_{\lambda c} = \tilde{\delta}_{\rho c} = \tilde{\delta}_{sc} = 2.5\%$. Temperature courses in the ceramic layer after heating time $t = 100$ s for the disturbed input data differ subtly from the courses for undisturbed data, which is presented in Fig. 3. The temperature course in the ceramic layer may be approximated with the linear function for $\delta_c = 0.1$ mm. Approximation by means of the polynomial of degree 2 and 3 imitates well the temperature course in the ceramic layer for $\delta_c = 0.2$ mm and $\delta_c = 0.3$ mm (Fig. 4), accordingly. In Fig. 4, the approximation functions are shown for the dimensionless ceramic layer thickness coordinate of the form

$$x = \frac{r_i - r_N}{r_{N+M} - r_N} \quad \text{for} \quad r_N \le r_i \le r_{N+M}\,. \tag{26}$$

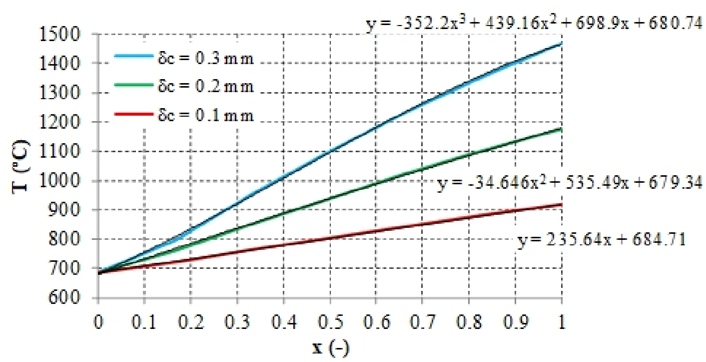

Figure 4: Temperature distribution in the ceramic layer for dimensionless coordinate after 100 s for the different thickness of the ceramic layer ($\delta_c = 0.1$ mm, 0.2 mm, and 0.3 mm) with undisturbed input data.

A basic difficulty in solving of the inverse problem discussed in this paper is its stability considering temperature measurement errors, as well as the disturbance errors of the thermophysical values of steel and zirconium dioxide. A stability measure of the discussed Cauchy problem, which is an ill posed problem [22], is the value of the spectral radius whose values for different numerical tests are presented in Figs. 5–8. The spectral radius values increase for the subsequent time units from the value of 0.21 to 0.28 for the ceramic layer thickness $\delta_c = 0.1$ mm (Fig. 5). As far as the zirconium dioxide layer $\delta_c = 0.2$ mm is concerned, the spectral radius values increase for the subsequent time units from the value of 0.39 to 0.51, and for $\delta_c = 0.3$ mm, they increase from 0.6 to 0.83 (Fig. 5). The spectral radius values below unities prove a stable solution of the inverse problem. A similar numerical test was carried out also for a high value of inner radius ($r_{\text{in}} = 50$ mm and $r_{\text{in}} = 100$ mm). In such a case, the cylindrical layer approaches the flat layer. Thus, the spectral radii of the stability matrix do not exceed the unity (Fig. 6). For all the cases under consideration, the input data disturbance did not cause significant changes in the spectral radius (Figs. 5–6).

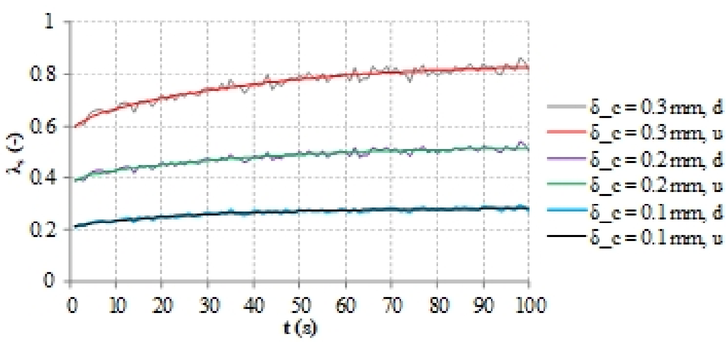

Figure 5: Spectral radius λ_s of stability matrix for the different thickness of the ceramic layer ($\delta_c = 0.1$ mm, 0.2 mm, and 0.3 mm) with disturbed (d) and undisturbed (u) input data.

The analysis covered the impact of the ceramic layer thickness δ_c (from 0.02 to 1 mm) on the spectral radius value with the assumed thickness of the double-layer area $g_{mc} = g + \delta_c$ (g_{mc} amounted to 5.1 mm, 5.2 mm or 5.3 mm) after the warm-up time of $t = 100$ s. The calculations were carried out for the cylindrical area with the radius of $r_{\text{in}} = 5$ mm (Fig. 7) and for the area close to the board with radius $r_{\text{in}} = 100$ mm (Fig. 8). For all the considered cases, the increase in the ceramic layer thickness is connected with the increase in the spectral radius, and the spectral radius courses in the thickness function of the zirconium dioxide layer for disturbed and undisturbed data differ in a negligible degree. The limit value of the spectral radius for which the considered inverse problem is numerically unstable is

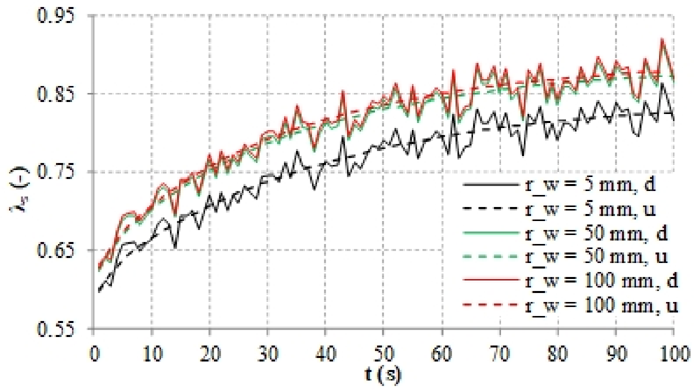

Figure 6: Spectral radius λ_s of the stability matrix for different internal radii (r_{in} = 5 mm, 50 mm, and 100 mm) and the constant thickness of the ring (g = 5 mm), the thickness of the ceramic layer $\delta_c = 0.3$ mm with disturbed (d) and undisturbed (u) input data.

$\lambda_s = 1$. The spectral radius was $\lambda_s = 1$ for the ceramic thickness $\delta_c = 0.93$ mm with the double-layer area thickness $g_{mc} = 5.1$ mm; $\delta_c = 0.68$ mm for $g_{mc} = 5.2$ mm and $\delta_c = 0.59$ mm for $g_{mc} = 5.3$ mm (for the inner radius $r_{\text{in}} = 5$ mm, Fig. 7). Similarly, ceramic thickness values for which the spectral radius reached the value of 1 amounted to $\delta_c = 0.86$ mm, $\delta_c = 0.63$ mm, and $\delta_c = 0.55$ mm, subsequently for $g_{mc} = 5.1$ mm, $g_{mc} = 5.2$ mm and $g_{mc} = 5.3$ mm with the inner radius $r_{\text{in}} = 100$ mm (Fig. 8).

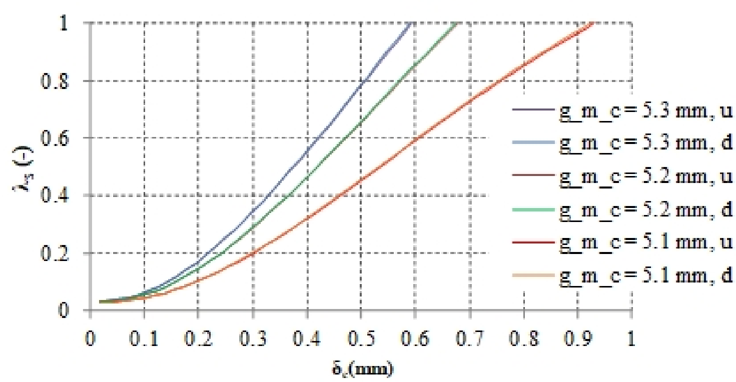

Figure 7: Spectral radius λ_s of the stability matrix for $r_{\text{in}} = 5$ mm for variable thickness double-layer area (g_{mc} = 5.1 mm, 5.2 mm, and 5.3 mm) and ceramic layer δ_c from 0.02 mm to 1 mm with disturbed (d) and undisturbed (u) input data.

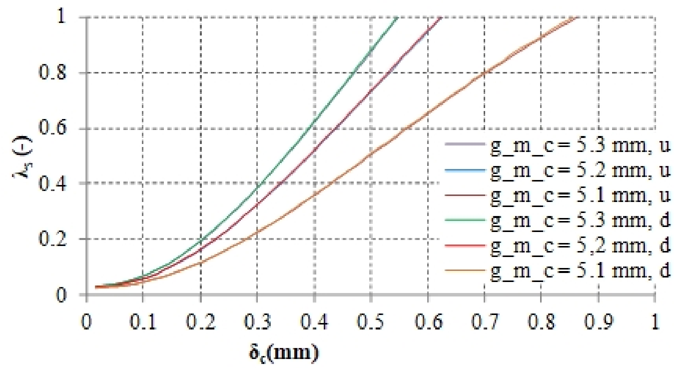

Figure 8: Spectral radius λ_s of the stability matrix for $r_{\text{in}} = 100$ mm for variable thickness double-layer area ($g_{mc} = 5.1$ mm, 5.2 mm, and 5.3 mm) and ceramic layer δ_c from 0.02 mm to 1 mm with disturbed (d) and undisturbed (u) input data.

4 Summary

The temperature control difficulty concerning the turbine blade coated with the protective ceramic layer with high heat load was overcome numerically in this paper. The permissible operating temperature was defined for the various thickness of the zircon dioxide layer (0.1, 0.2, and 0.3 mm) for the assumed maximum steel temperature at the level of 686°C. The calculations were carried out for undisturbed data and randomly disturbed data up to the value of 0.5% for the temperature and 2.5% for the thermophysical properties. In both cases stable results were obtained for the temperature distribution, which were subsequently interpolated with the polynomial function. Increasing the ceramic layer thickness ensures the possibility of the turbine blade operation in a higher temperature without a risk of exceeding the permissible thermal resistance of the metal.

The regularization method proposed in this paper based on the notation of the thermal balance for ceramic proved to be effective for the solution of the Cauchy problem. The suggested solution does not introduce a regularization parameter. Thus, we avoid using additional algorithms for determining its optimal value. The spectral radius of the equation matrix proves to be a good measure in the stability assessment of solutions. The change in time of the spectral radii for various geometry was presented in the paper. Notwithstanding the introduction of data disturbance in each of the analysed cases, the results obtained ranged within the solutions for undisturbed data. Furthermore, the value of spectral radii in the function of ceramic thickness was investigated. Both for undisturbed and disturbed data the results obtained were stable.

The essence of the presented paper was the determination of the temperature on the ceramic surface in the thickness function of the ceramic layer with consideration of the non-linear courses of thermophysical properties and their measurement errors. The thermal conductivity equation is satisfied in each inner point of the ceramic layer; nevertheless, the solution of the inverse problem, defining this temperature, is stable for the ceramic layer thickness $\delta_c < \delta_{c\_\max}$. The value of the spectral radius of the stability matrix was investigated in this paper for the subsequent values of the ceramic layer for which the spectral radius λ_s of the stability matrix satisfies the inequality $\lambda_s < 1$. The calculations carried out show, Figs. 3 and 4, that the temperature course in the ceramic layer is a linear function in relation to the ceramic thickness for $\delta_c < 0.1$ mm, square function for $\delta_c < 0.2$ mm and cubic function for $\delta_c < 0.3$ mm.

The proposed algorithm is an effective tool for the temperature control of the metal coated with a ceramic protective layer. It may be used for the thermal analysis of the elements exposed to a high thermal load, such as small arms barrels and combustion chambers.

Received 20 November 2023

References

[1] Ciupek B., Gołoś K., Jankowski R., Nadolny Z.: *Effect of hard coal combustion in water steam environment on chemical composition of exhaust gases.* Energies **14**(2021) 20, 6530-1–6530-24. doi: 10.3390/en14206530

[2] Grzymisławski P., Czyżewski P., Ślefarski R.: *Nitrogen dilution effect on swirl stabilized methane burning in gas turbine conditions.* Heat Transfer Eng. **44**(2023), 11-12, 1053–1060. doi: 10.1080/01457632.2022.2113443

[3] Joachimiak D.: *Novel method of the seal aerodynamic design to reduce leakage by matching the seal geometry to flow conditions.* Energies **14**(2021), 23, 7880-1–7880-16. doi: 10.3390/en14237880

[4] Joachimiak D., Frąckowiak A.: *Experimental and numerical analysis of the gas flow in the axisymmetric radial clearance.* Energies **13**(2020), 21, 5794-1–5794-13. doi: 10.3390/en13215794

[5] Joachimiak D., Krzyślak P.: *Experimental research and CFD calculations based investigations into gas flow in a short segment of a heavily worn straight through labyrinth seal.* Pol. Marit. Res. **24**(2017), 2, 83–88. doi: 10.1515/pomr-2017-0053

[6] Joachimiak M., Joachimiak D., Ciałkowski M.: *Investigation on thermal loads in steady-state conditions with the use of the solution to the inverse problem.* Heat Transfer Eng. **44**(2023), 11-12, 963–969. doi: 10.1080/01457632.2022.2113451

[7] Frąckowiak A., Ciałkowski M., Wróblewska A.: *Application of iterative algorithms for gas-turbine blades cooling optimization.* Int. J. Therm. Sci. **118**(2017), 198–206. doi: 10.1016/j.ijthermalsci.2017.04.016

[8] Frąckowiak A., von Wolfersdorf J., Ciałkowski M.: *Optimization of cooling of gas turbine blades with channels filled with porous material.* Int. J. Therm. Sci. **136**(2019), 370–378. doi: 10.1016/j.ijthermalsci.2018.09.005

[9] Frąckowiak A., von Wolfersdorf J., Ciałkowski M.: *Solution of the inverse heat conduction problem described by the Poisson equation for a cooled gas-turbine blade.* Int. J. Heat Mass Tran. **54**(2011), 5-6, 1236–1243. doi: 10.1016/j.ijheatmasstransfer.2010.11.001

[10] Ciałkowski M., Olejnik A., Joachimiak M., Grysa K., Frąckowiak A.: *Cauchy type nonlinear inverse problem in a two-layer area.* Int. J. Numer. Method. H. **32**(2022), 1, 313–331. doi: 10.1108/HFF-09-2020-0584

[11] Ciałkowski M., Olejnik A., Frąckowiak A., Lewandowska N., Mosiężny J.: *Cauchy type inverse problem in a two-layer area in the blades of gasturbine.* Energy **212**(2020), 118751. doi: 10.1016/j.energy.2020.118751

[12] Solekhudin I., Azis M.I.: *A dual reciprocity method for a class of heat conduction problems in two-layered materials.* Int. J. Comput. Sci. **50**(2023), 1, 1–10.

[13] Joachimiak M., Ciałkowski M., Frąckowiak A.: *Stable method for solving the Cauchy problem with the use of Chebyshev polynomials.* Int. J. Numer. Method. H. **30**(2020), 3, 1441–1456. doi: 10.1108/HFF-05-2019-0416

[14] Joachimiak M., Ciałkowski M.: *Influence of the heat source location on the stability of the solution to the Cauchy problem.* E3S Web Conf. **323**(2021), 00016, 1–2. doi: 10.1051/e3sconf/202132300016

[15] Ciupek B., Judt W., Gołoś K., Urbaniak R.: *Analysis of low-power boilers work on real heat loads: A case of Poland.* Energies **14**(2021), 11, 3101-1–3101-13. doi: 10.3390/en14113101

[16] Judt W., Ciupek B., Urbaniak R.: *Numerical study of a heat transfer process in a low power heating boiler equipped with afterburning chamber.* Energy **196**(2020), 117093. doi: 10.1016/j.energy.2020.117093

[17] Taler J., Weglowski B., Pilarczyk M.: *Monitoring of thermal stresses in pressure components using inverse heat conduction methods.* Int. J. Numer. Method. H. **27**(2017), 3, 740–756. doi: 10.1108/HFF-03-2016-0091

[18] Joachimiak M., Ciałkowski M., Bartoszewicz J.: *Analysis of temperature distribution in a pipe with inner mineral deposit.* Arch. Thermodyn. **3**5(2014), 2, 37–49. doi: 10.2478/aoter-2014-0012

[19] Zieliński M., Koniorczyk P., Surma Z., Zmywaczyk J., Preiskorn M.: *Numerical study of heat transfer in a gun barrel made of selected steels.* Energies 15(2022), 1868, 1–24. doi: 10.3390/en15051868

[20] Brodzik Ł., Frąckowiak A.: *Optimization of the heat flow by solving inverse problem in the protective layer of the TPS panel*. Int. J. Numer. Method. H. **30**(2020), 6, 2989–3003. doi: 10.1108/HFF-12-2018-0749

[21] Chung S.Y.: *Uniqueness in the Cauchy problem for the heat equation*. P. Edinburgh Math Soc. **42**(1999), 455–468.

[22] Hadamard J.: *Lectures on Cauchy's Problem in Linear Partial Differential Equations*. Dover Publ., New York 1953.

[23] Joachimiak M., Ciałkowski M.: *Optimal choice of integral parameter in a process of solving the inverse problem for heat equation*. Arch. Thermodyn. **35**(2014), 3, 265–280.

[24] Mierzwiczak M., Kołodziej J.A.: *The determination of heat sources in two dimensional inverse steady heat problems by means of the method of fundamental solutions*. Inverse Probl. Sci. En. **19**(2011), 6, 777–792. doi: 10.1080/17415977.2010.539685

[25] Mierzwiczak M., Kołodziej J.A.: *The determination temperature-dependent thermal conductivity as inverse steady heat conduction problem*. Int. J. Heat Mass Tran. **54**(2011), 4, 790–796. doi: 10.1016/j.ijheatmasstransfer.2010.10.024

[26] Payne L.E., Philippin G.A.: *An ill-posed problem for the heat equation*. Math. Mod. Meth. Appl. S. **19**(2009), 9, 1631–1641.

[27] Belgacem F.B.: *Why is the Cauchy problem severely ill-posed?* Inverse Probl. **23**(2007), 2, 823–836.

[28] Joachimiak M., Ciałkowski M.: *Non-linear unsteady inverse boundary problem for heat conduction equation*. Arch. Thermodyn. **38**(2017), 2, 81–100. doi: 10.1515/aoter-2017-0011

[29] Joachimiak M., Ciałkowski M.: *Stable solution to nonstationary inverse heat conduction equation*. Arch. Thermodyn. **39**(2018), 1, 25–37. doi: 10.1515/aoter-2018-0002

[30] Mierzwiczak M., Chen W., Fu Z.-J.: *The singular boundary method for steady-state nonlinear heat conduction problem with temperature-dependent thermal conductivity*. Int. J. Heat Mass Tran. **91**(2015), 205–217. doi: 10.1016/j.ijheatmasstransfer.2015.07.051

[31] Jaremkiewicz M., Taler J.: *Online determining heat transfer coefficient for monitoring transient thermal stresses*. Energies **13**(2020), 3, 704, 1–13. doi: 10.3390/en13030704

[32] Joachimiak M.: *Analysis of thermodynamic parameter variability in a chamber of a furnace for thermo-chemical treatment*. Energies **14**(2021), 10, 2903, 1–18. doi: 10.3390/en14102903

[33] Joachimiak M., Joachimiak D.: *Analysis of heating time and of temperature distributions for cylindrical geometry with the use of solution to the inverse problem*. E3S Web Conf. **323**(2021), 00013, 1–4. doi: 10.1051/e3sconf/202132300013

[34] Joachimiak M., Joachimiak D.: *Modelling of the cylindrical geometry cooling process based on the solution of the inverse problem*. E3S Web Conf. **321**(2021), 02017, 1–5.

[35] Joachimiak M., Joachimiak D., Ciałkowski M., Małdziński L., Okoniewicz P., Ostrowska K.: *Analysis of the heat transfer for processes of the cylinder heating in the heat-treating furnace on the basis of solving the inverse problem*. Int. J. Therm. Sci. **145**(2019), 105985, 1–11. doi: 10.1016/j.ijthermalsci.2019.105985

[36] Engl H.W., Hanke M., Neubauer A.: *Regularization of Inverse Problems. Mathematics and its Applications*. Kluwer, Dordrecht 1996.

[37] Hansen P.C.: *Regularization tools: a Matlab package for analysis and solution of discrete ill-posed problems*. Numer. Algorithms **6**(1994), 1-2, 1–35.

[38] Joachimiak M.: *Choice of the regularization parameter for the Cauchy problem for the Laplace equation*. Int. J. Numer. Method. H. **30**(2020), 10, 4475–4492. doi: 10.1108/HFF-10-2019-0730

[39] Tikhonov A.N., Arsenin V.Y.: *Solution of Ill-Posed Problems*. Wiley, New York 1977.

[40] Hasanov A., Mukanova B.: *Relationship between representation formulas for unique regularized solutions of inverse source problems with final overdetermination and singular value decomposition of input-output operators*. J. Appl. Math. **80**(2015), 3, 676–696.

[41] Hansen P.C.: *Discrete Inverse Problems: Insight and Algorithms*. SIAM, Philadelphia 2010.

[42] Marin L.: *Numerical solution of the Cauchy problem for steady-state heat transfer in two-dimensional functionally graded materials*. Int. J. Solids Struct. **42**(2005), 4338–4351.

[43] Wang M., Troesch, A.W.: *Numerical stability analysis for free surface flows*. Int. J. Numer. Meth. Fl. **24**(1997), 893–912.

[44] Joachimiak M., Frąckowiak A., Ciałkowski M.: *Solution of inverse heat conduction equation with the use of Chebyshev polynomials*. Arch. Thermodyn. **37**(2016), 4, 73–88. doi: 10.1515/aoter-2016-0028

[45] Joachimiak D., Judt W., Joachimiak M.: *Numerical analysis of the heating of a die for the extrusion of aluminium alloy profiles in terms of thermochemical treatment*. Arch. Thermodyn. **44**(2023), 2, 159–175. doi: 10.24425/ather.2023.146563

[46] Ciałkowski M., Joachimiak M., Mierzwiczak M., Frąckowiak A., Olejnik A., Kozakiewicz A.: *Cauchy type nonlinear inverse problem in a two-layer cylindrical area*. Heat Transfer Eng. (*in print*)